Conference paper

Hyo Seung Park, Su Yeon Lee, Hyunsik Yoon and Insup Noh*

Biological evaluation of micro-patterned hyaluronic acid hydrogel for bone tissue engineering

Abstract: Design of micro-patterning of hydrogel is of critical importance in both understanding cellular behaviors and mimicking controlled microenvironments and architectures of diverse well-organized tissues. After micro-patterning of hyaluronic acid (HA) hydrogel on a poly(dimethyl siloxane) substrate, its physical and biological properties have been compared with those of a non-patterned hydrogel for its possible applications in bone tissue engineering. The micro-patterned morphologies of HA hydrogel in both swollen and dehydrated forms have been observed with light microscope and scanning electron microscope, respectively, before and after *in vitro* cell culture. When MC3T3 bone cells were *in vitro* cultured on both HA hydrogels, the micro-patterned one shows excellence in cell proliferation and lining for 7 days along the micro-pattern paths over those of the non-patterned one, which have shown less cell-adhesiveness. The cytotoxicity of the micro-patterned HA hydrogels was *in vitro* evaluated by the assays of MTT, BrdU and Neutral red. The viability and morphology of MC3T3 cells on both HA hydrogels were observed with a fluorescence microscope by the live & dead assay, where their viability was confirmed by staining of F-actin development. The results of their H&E staining showed that both micro-patterned and non-patterned hydrogels induced development of tissue regeneration as observed by cell attachment, proliferation, and survivability, but the micro-patterned one induced distinctive patterning of both better initial cells adhesion on the micro-patterns and subsequently development of their proliferation and extracellular matrix, which were considered as important characteristics in their applications to tissue engineering.

Keywords: biocompatibility; hyaluronic acid; hydrogel; ICFPAM 2013; micro-pattern.

DOI 10.1515/pac-2014-0613

Article note: A Special Topic article based on a presentation at the 12th International Conference on Frontiers of Polymers and Advanced Materials (ICFPAM 2013), Auckland, New Zealand, 8–13 December 2013.

***Corresponding author: Insup Noh,** Department of Chemical Engineering, Seoul National University of Science and Technology, 232 Gongneung-ro, Nowon-gu, Seoul 139-743 Korea (Republic of Korea); and Convergence Institute of Biomedical Engineering and Biomaterials, Seoul National University of Science and Technology, 232 Gongneung-ro, Nowon-gu, Seoul 139-743 Korea (Republic of Korea), Tel.: +822-970-6603, Fax: +822-977-8317, E-mail: insup@seoultech.ac.kr

Hyo Seung Park and Su Yeon Lee: Department of Chemical Engineering, Seoul National University of Science and Technology, 232 Gongneung-ro, Nowon-gu, Seoul 139-743 Korea (Republic of Korea); and Convergence Institute of Biomedical Engineering and Biomaterials, Seoul National University of Science and Technology, 232 Gongneung-ro, Nowon-gu, Seoul 139-743 Korea (Republic of Korea)

Hyunsik Yoon: Department of Chemical Engineering, Seoul National University of Science and Technology, 232 Gongneung-ro, Nowon-gu, Seoul 139-743 Korea (Republic of Korea)

Introduction

Micro-patterning of polymeric biomaterials has been reported by various techniques such as microfluidics [1–3], lab-on-chip [2–4], soft lithography [5–7], micro-contact printing [8–14] and micro-molding [15]. Micro-patterning has drawn interesting to researchers in both science and technology. While its scientific interesting would be understanding a relationship between the micro-structures of scaffolds and the host tissues, technological interesting would be high possibilities of its applications to regeneration of various tissues such as bone [16, 17], cartilage [18, 19], bladder [20] and blood vessels [15, 21]. Examples of micro-patterning techniques in tissue engineering could be possibilities of precise fabrications of complicated scaffolds, leading to mimicking of the structural architectures of to-be-replaced human tissues and organs. Applications of these micro-patternings to diverse tissue engineering have expanded the scope of their applications to the areas of Bio-MEMS [22, 23], μ-TAS [1, 24], Lap on chip [2–4] and biosensors [22, 24] among others.

Hydrogel has been recognized as an important scaffold in tissue engineering due to its unique characteristics such as high water content, minimal immune-responses and mechanical and biochemical properties similar to those of body tissues [25, 26]. Numerous polymers such as hyaluronic acid, chondroitin sulfate, poly(vinyl alcohol), poly(ethylene oxide), collagen, alginate, dextran and chitosan have been employed as hydrogel polymers for tissue engineering [27]. Hyaluronic acid (HA) among those polymeric biomaterials has attracted high interests in its employment in tissue regenerations due to its unique properties such as ubiquitous existence as natural extra-cellular matrix throughout the human body, and its physico-chemical and immune-neutral properties [28]. These advantageous properties led to development of diverse HA hydrogels to commercially available medical devices such as dermal fillers [29, 30] and scaffolds for regeneration of blood vessel [31, 32], bone and cartilage [33–35] as well as wound healing [36–38].

Advantages of HA hydrogel in its applications to micro-patterning techniques would be fabrication of layer-by-layer biocompatible scaffolds in 3-D architectures, and encapsulation and local delivery of both cells and bioactive agents to adjacent host tissues. Fabrications and characterizations of biocompatible micro-patterned HA hydrogels would give foresights in understating of tissue engineering mechanisms and designing of cellular behaviors-based tissue engineering scaffolds, since the cells in the body have been well organized in complex tissues and organs, being influenced to a large extent by the surrounding micro-environments. Keeping the morphologies of the micro-patterns of hydrogels in cell culture medium would be very important to micro-environment experiments. If the micro-patterns swell too much, the substrates are no longer micro-environments and the adhered cells might behave differently, losing validation of this micro-pattern experiment. We here reported fabrication of micro-patterning of HA hydrogel using the PDMS substrates and then evaluation of its biocompatibility for bone tissue engineering, by keeping the morphologies of micro-patterns during cell cultures. After evaluation of the micro-patterned HA hydrogel by light microscope and SEM, its biocompatibility and cytotoxicity were performed with MC3T3 cells on both the micro-patterned and non-patterned HA hydrogel for 7 days. The results showed that all the cells were viable and well proliferated on both the micro-patterned and non-patterned hydrogels, but the micro-patterned one induced higher cell adhesion and proliferation and better cellular responses for bone-tissue engineering.

Materials and methods

Materials

Hyaluronic acid (HA) (MW: 575 kDa) was donated by Hanmi Pharmaceutical Co. (Pyeongtaek, Korea). While 1,4-butanediol diglycidyl ether (MW: 202 Da), Mayer's Hematoxylin solution and the Eosin (H&E) Y solution, alcohol and α-MEM were purchased from Sigma-Aldrich (MO, USA), sodium hydroxide (MW: 40 Da) was bought from Yakuri Pure Chemical Co. (Kyoto, Japan). Poly(dimethyl siloxane) (PDMS) (184 Sylgard) was purchased from Dow Corning Korea (Seoul, Korea). While penicillin-streptomycin was purchased from Lonza Korea (Seoul, Korea), cell counting kit-8 (CCK-8) solution was bought from Dojindo Laboratories (Kumamoto,

Japan) through Biomax Co., Ltd. (Seoul, Korea). Both F-actin staining kit and live & dead viability/cytotoxicity kit for mammalian cells were purchased from Invitrogen (CA, USA) through Life Technology Korea (Seoul, Korea), and bovine serum albumin (BSA) was purchased from R&D systems (USA). *In vitro* toxicology assay kits such as assay kits of bromodeoxyuridine (BrdU), thiazolyl blue tetrazolium bromide (MTT) and Neutral red were purchased from Sigma-Aldrich (MO, USA), Roche Korea Co. (Seoul, Korea) and Life Technology Korea (Seoul, Korea), respectively. All chemicals were employed as received.

Fabrication of the prism shaped replica mold

The replica mold used was prepared from a metallic master fabricated mechanically as reported in previous [39]. In brief, we prepared a blank plate of stainless steel electroplated by nickel. Then, the plate surface was machined by a diamond cutting tool with an angle of 45° and an interval of 20 μm. After the preparation of the metallic masters, drops of an UV-curable poly(urethane acrylate) (PUA; 301RM, Minuta Tech, Korea) prepolymer were dispensed onto the master mold, and a flexible backplane film was placed on top of them. After exposing the PUA prepolymer UV light, the cross-linked polymeric replica mold (10 cm × 10 cm) was removed from the original master.

Fabrication of micro-patterned/non-patterned HA hydrogel

A master mold with a specific form was fixed on a polystyrene petridish by a dual tape (Fig. 1a). The PDMS (Sylgard 184 Silicone elastomer base: Sylgard R 184 Silicone elastomer curing agent = 10: 1 ratio) was mixed fully. This solution was poured on the fixed master and put on flat place for 1 day at room temperature to remove bubbles, then it was put on the place overnight at 60 °C. After curing the PDMS mold (7.5 cm × 2.5 cm) and then separating from a master mold, it was used to fabricate a micro-patterned HA hydrogel (d = 1 cm) (Fig. 1b). After mixing HA solution (18 % w/v) in 1 % NaOH solution for about 1 hr at room temperature, butanediol diglycidyl ether (BDDE) was added in the mixture solution. After controlling the concentrations of the BDDE cross-linkers at 400 μL/g (BDDE/HA), the solution was injected though each PDMS mold by a 1 mL syringe. After filling the mixture solution in the PDMS mold completely (Fig. 1c), the cross-linked hydrogels was removed from the PDMS mold after 24 h (Fig. 1d). The volume of HA hydrogel was measured as approximately 80 μL. After soaking the hydrogel in 100 % ethanol for 1 d, it was washed in phosphate buffered solution (PBS) solution for 3 d by exchanging the PBS solution with fresh one every 12 h.

Attenuated total reflectance Fourier transform infrared spectroscopy (ATR-FTIR)

To confirm cross-linking of HA polymers, i.e., formation of HA hydrogel, ATR-FTIR spectra of both HA polymer (0.01 g) and HA hydrogel powder (0.01 g) were recorded at a wavelength of 650–4000 cm^{-1} with a spectrom-

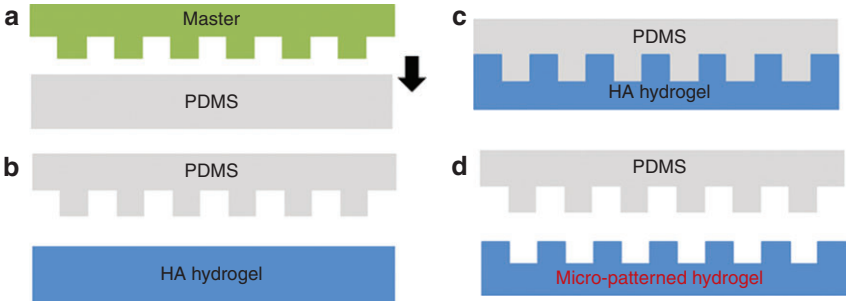

Fig. 1 Schematic diagram of micro-patterning of HA hydrogel.

eter (Travel IR; Smiths, USA). While a refractive index of a diamond crystal was measured as 2.4 at a 45° incidence angle, the ATR depth of penetration was done as about 2 μm [40].

Swelling

After measuring the weight of the obtained hydrogel with a microbalance, swelling of HA- hydrogel was determined by comparing the weight of HA hydrogels immersed in PBS over time. The weight of HA hydrogel was measured by immersing it in PBS at pH 7.4. Adherent water was removed by blotting the wet HA hydrogels with a piece of Kimwipe paper before weighing them on an electronic balance. The percentage of hydrogel swelling was calculated by using a following formula at room temperature.

$$\text{Swelling} = \frac{W_s - W_i}{W_i} \times 100(\%)$$

Where W_s and W_i are the wet weights of the HA hydrogels at time t and at initial gelation point, respectively [41].

In vitro cell culture

An osteoblast precursor cell lines derived from Mus musculus (mouse) calvaria (MC3T3) (< 15 passage) were *in vitro* cultured in α-MEM media containing both 10 % fetal bovine serum (Gibco Korea, Korea) and penicillin-streptomycin (100 unit/mL) in an *in vitro* incubator with 5 % CO_2 at 37 °C. After sterilization of the hydrogel (diameter = 1 cm, thickness = 1 mm) by autoclave (AC-02, Jeio Tech; Seoul, Korea), the cells were cultured on the surfaces of both the micro-patterned and non-patterned HA hydrogel at the density of 50 000 cells/surface for 7 d.

Cell adhesion and proliferation were evaluated with the assay of the cell counting kit-8 (CCK-8, Dojindo, Japan) after seeding MC3T3 cells on the surface of the HA hydrogel. The cell number was counted as below with the CCK-8 assay kit and a microplate reader (Genios Basic; Tecan Korea; Seoul, Korea). 100 μL CCK-8 solution was inserted into the 900 μL α-MEM medium and then the cell culture plate with samples was inserted in the *in vitro* CO_2 incubator. After 2 h, 100 μL medium with CCK-8 solution was aliquoted into a 96 well plate and an optical density of the CCK-8 loaded medium was measured at the wavelength of 450 nm by the microplate reader.

Morphological analysis

The morphologies of HA hydrogel were visualized by a scanning electron microscopy (SEM; Tescan VEGA3; Kohoutovice, Czech Republic) after processing of dehydration and gold-sputter coating of the HA hydrogel as follows. The swollen hydrogel samples (diameter = 10 mm, thickness = 1 mm) were frozen in liquid nitrogen for 30 min and then freeze-dried at −82 °C for 4 d by a freeze dryer (FD-8508, Ilshin Bio Base, Korea). The dry samples were mounted on an aluminum stub with a double-sided tape, and then gold-coated in vacuum for 1 min. The morphology of the dehydrated gold-coated HA hydrogels were analyzed with SEM. *In vitro* cells cultured on the HA hydrogel was fixed in 2.5 % glutaraldehyde for 1d and washed with PBS for l d. Their morphological observation of the washed samples was done as before.

Live & dead assay

In vitro cell viability and adhesions on both the surface of the micro-patterned and non-patterned HA hydrogel were observed with MC3T3 cells in a 24-well cultured plate. Assay of live & dead viability/cytotoxicity for

mammalian cells was processed according to the protocol suggested by the vendor (Invitrogen, USA), by adding the solutions of both 1.2 μL of 2 mM ethidium homodimer-1 (EthD-1) and 0.3 μL of 4 mM calcein AM into 600 μL PBS. After addition of the prepared HA hydrogel in the prepared agents and then 30 min incubation in the *in vitro* incubator, cell viability on the HA hydrogel was observed by a fluorescence microscope (Leica DMLB, Germany).

F-actin staining

MC3T3 cells cultured on the surface of the micro-patterned and non-patterned HA hydrogels for 7 d in the 24-well cultured plate were fixed in 4 % formaldehyde for 10 min, and then in 0.1 % solution of Triton X-100 in PBS for 5 min. The prepared samples were soaked in 1 % BSA solution for 20 min. For staining with phallotoxin, the F-actin solution was made by diluting 10 μL F-actin solution into 200 μL PBS, and then the samples were soaked in the F-actin solution for 20 min. F-actin on the hydrogel was observed by a fluorescence microscope (Leica DMLB, Germany).

H&E staining

The samples cultured for 7 d in the 24 well-plate were fixed in 4 % formaldehyde solution for 10 min, and then washed with PBS for 5 min. The samples were stained with H&E solution by soaking them in the diluted mixture solution of 500 μL Mayor's hematoxylin stain solution and 500 μL distilled water for 30 s and then in the eosin stain solution for 3 min. The stained samples were visualized with a light microscopy (CKX41; Olympus, Japan).

Evaluations of cytotoxicity

Thiazoly blue tetrazolium bromide (MTT assay)

After seeding MC3T3 cells in a 96 well-plate at a density of 1×10^4 cells, *in vitro* cell culture lasted in a 5 % CO_2 incubator at 37 °C for 24 h, and then the medium was removed. Three kinds solutions of 100 μL from each 1 mL extract that was obtained from the culture medium of HA hydrogel, Teflon and Latex (1 × 1 cm) for 72 h were added into the cell culture media for another 24 h. Cell culture lasted for another 4 h after addition of 20 μL MTT solution (2 mg/mL in PBS) in the culture medium, and then sequential removals of the culture medium and addition of 100 μL dimethylsulfoxide (DMSO) followed. The optical density of the final solution was measured by the microplate reader at a wavelength of 570 nm.

Neutral red assay

Three kinds of extracts from the HA hydrogel, Teflon and Latex were prepared after loading the samples in the cell culture medium (1 mL) for 72 h 100 μL of extracts of the samples was dispensed into cells. *In vitro* cell culture lasted in 5 % CO_2 incubator at 37 °C for 24 h after seeding MC3T3 cells at a density of 1×10^4 cells/well. The medium was removed from the well, and then cell culture lasted for another 24 h after addition of the prepared extract solution. Subsequent to addition of the culture medium and 0.33 % Neutral red solution at a ratio of 9:1 in the *in vitro* incubator, cell culture lasted for another 2 h. After washing with the fixation solution of the assay and then proceeding reaction for 10 min, addition of 100 μL solubilization solution was done on each well. Its optical density was measured at an absorbance wavelength of 550 nm by the microplate reader by referencing the wavelength of 690 nm.

Bromodeoxyuridine (BrdU) assay

MC3T3 cells at a density of 1×10^4 cells were cultured in a 96-well culture well plate for 24 h, after loading 100 μL from the 1 mL extract solution of the HA hydrogel. 10 μL BrdU labeling solution was added into the culture medium and then *in vitro* cell culture lasted for another 2 h. After removing the labeling medium, 200 μL Fixdent solution and 100 μL anti-BrdU peroxide-labeled anti-BrdU antibody per well was added according to the manufacturer's protocol. After washing the wells, 25 μL 1 M H_2SO_4 solution was added into each well, and then optical density was measured at the absorbance wavelength of 450 nm by microplate reader by referring to that of 690 nm.

Statistical analysis

Data were expressed as mean ± standard deviations. Statistical significance was assessed with one-way and multi-way ANOVA by employing the SPSS 18.0 program (ver. 18.0, SPSS Inc., Chicago, IL, USA). The comparisons between two groups were carried out using a t-test. The samples were considered as significantly different when $p < 0.05$.

Results

ATR-FTIR

FTIR spectrum showed characteristic peaks of HA such as –OH stretch vibration and –NH symmetrical vibration at 3300 cm^{-1}; amide I carbonyl (C=O) at 1600 cm^{-1}; C–O–H deformation vibration at 1400 cm^{-1}, $-CH_3$ deformation vibration at 1300 cm^{-1}, C–O–C stretching vibration at 1130 cm^{-1}, –CH–O–CH– stretching vibration at 1030 cm^{-1} (Fig. 2A). The spectrum of HA hydrogel showed new peaks of C–C–O–C–C at the wavelength of 990 and 815 cm^{-1} (Fig. 2B-a,b,c).

Characterizations of microstructures

After observing the surfaces of the master, PDMS and micro-patterned HA hydrogel by optical microscope, the diameters of patterns on the HA hydrogels were measured with an image analyzer. The diameters of the

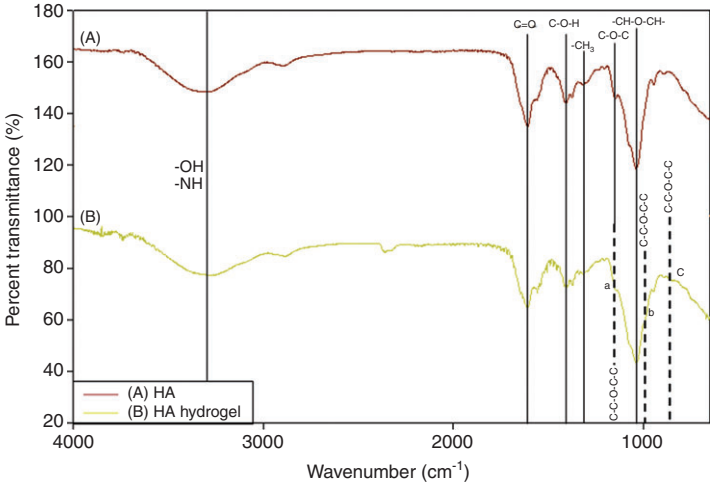

Fig. 2 FTIR spectra of HA polymer (A) and HA hydrogel (B), where new peaks (b,c) were observed after formation of hydrogel.

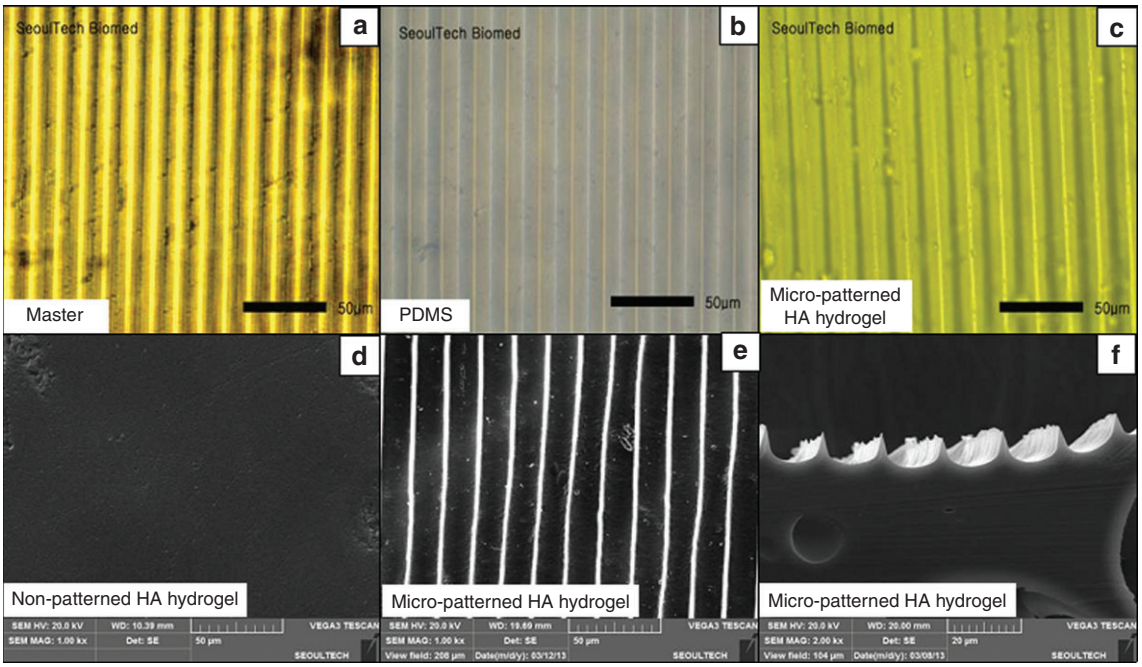

Fig. 3 Optical images (a-c; ×400) of the molds of (a) master, (b) PDMS and (c) micro-patterned HA hydrogel after swelling in PBS for 24 h; and SEM images (d and e, ×1000 and F, ×2000) of HA hydrogel with either non-pattern (surface, d) or micro-patterns [surface (e) and X-section (f)].

master and PDMS were measured as 14.9 ± 0.9 μm and 19.6 ± 0.4 μm, respectively (Fig. 3a, b). Micro-patterned HA hydrogel showed the diameter of semi-circles similar to those of the master and PDMS even after its swelling for 24 h in PBS buffer (pH 7.4), i.e., about 19.8 ± 0.2 μm (Fig. 3c). Both non-patterned and micro-patterned HA hydrogels showed formation of smooth and localized micro-patterned surfaces, respectively, as observed by SEM (Fig. 3d, e). The cross-sections of the micro-patterned HA hydrogel had a semicircle shape with a dimension of 17.5 ± 0.1 μm to 8.5 ± 0.1 μm in diameter and height, respectively (Fig. 3f).

Swelling of micro-patterned HA gel

Swelling of the HA hydrogel were measured for the samples both with and without micro-patterning process. The non-patterned HA hydrogels showed very high swelling behaviors in pH 10, i.e., approximately 10 times increase in their weights after immersion for 2 days (Fig. 4), but the micro-patterned HA hydrogel showed preservation of micro-patterns on its surface, obtaining a dehydrated micro-patterned hydrogel with a dimension of 17.5 μm in diameter and 2.4 μm in height by SEM as we have shown in Fig. 3f. The dimension of these HA hydrogels did not change even during *in vitro* cell culture for 7 days (see below Fig. 7 in detail), where the final diameter of micro-pattern was measured as 20.5 μm. These results indicated that swelling of the micro-patterned HA hydrogel induced 13.1 and 17.1 % increases of the diameters of micro-patterns after their immersion in distilled water for 1 h and in cell culture medium for 7 days, respectively.

Effect of micro-patterns on cell behaviors

To see the effect of micro-patterns on cell proliferation on the HA hydrogel, the HA hydrogels with micro-pattern and non-pattern were evaluated by counting the cell numbers with CCK-8 assay at day 1, 3 and 7 after seeding MC3T3 cells at a loading density of 50 000 cells per HA hydrogel for 7 days. While the cell numbers

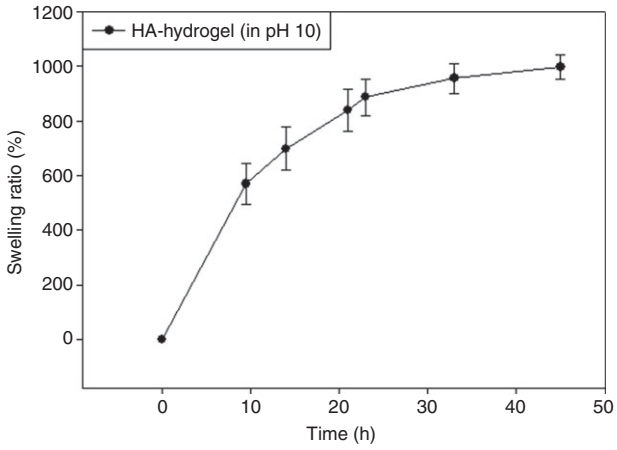

Fig. 4 Swelling behaviors of non-patterned HA hydrogel in pH 10.

of the non-patterned HA hydrogel showed increase in cell numbers from 0.18 ± 0.02 to 0.24 ± 0.03 at day 1 and 7, those of the micro-patterned one did 0.23 ± 0.04–0.32 ± 0.05, correspondingly (Fig. 5a). These results indicated that even though there were no significant differences in statistics between the values of optical density of the micro-patterned and non-patterned HA hydrogels, increases in cell proliferation on the micro-patterned HA hydrogel was clearly observed by normalizing their cell numbers of day 3 and 7 by the value of the number of initially adhered cells at day 1. In specific, while the proliferations of cells adhesion on the non-patterned hydrogels were measured as 117 ± 12 and 139 ± 32 % for 3 and 7 days, those of the micro-patterned ones were 126 ± 33 and 146 ± 42 %, respectively (Fig. 5b). The results showed no significant difference in statistics.

In vitro cytotoxicity of HA hydrogel by the assays of MTT/Neutral Red/BrdU

In vitro biocompatibility of HA hydrogels was evaluated by measuring cytotoxicity of specific cell organs by the assays of MTT, Neutral Red and BrdU by using the extracts of HA micro-patterned hydrogels (Fig. 6). The assays were to observe the effects of the extracts of the HA hydrogel substrates on possible damages to mitochondria, lysosome and deoxyribonucleic acid, correspondingly, where the extracts were obtained by immersing the samples in buffer solution for 3 days. The degrees of MC3T3 cytotoxicity of the HA hydrogels were measured and then compared the values of their optical densities with those of both Teflon and Latex.

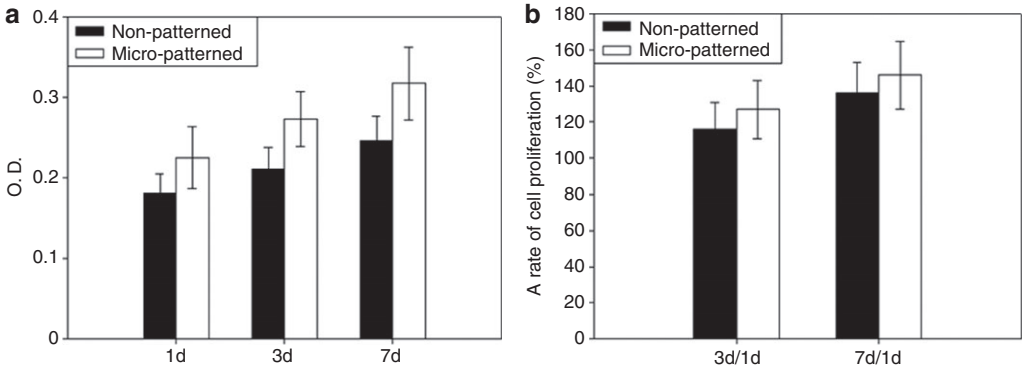

Fig. 5 (a) Proliferation of MC3T3 cells on the HA hydrogels *in vitro* cell cultured for 7 days with either non-pattern or micro-pattern; (b) their proliferation ratios by normalizing the cell numbers at day 1.

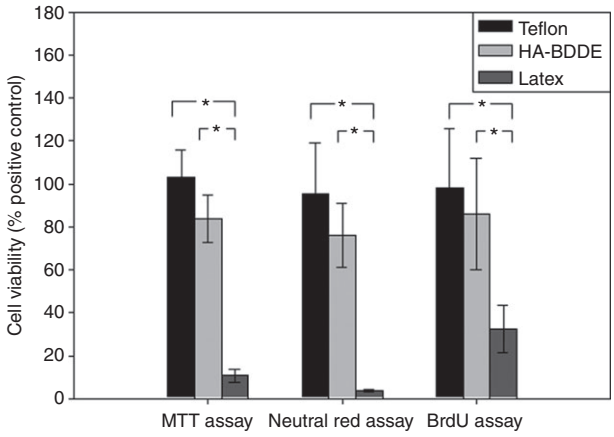

Fig. 6 Cytotoxicity of HA-BDDE hydrogel with MC3T3 cells by the assays of MTT, Neutral Red and BrdU. Teflon and Latex were employed as positive and negative controls, respectively, and the value of optical density of the culture medium was considered as 100 %.

Teflon and Latex were employed as positive and negative controls, respectively, and the value of cell culture medium was considered as 100 %. The HA hydrogels showed much better biocompatibility of cell organs than the Latex did. In specific, while relative cell viabilities of the HA hydrogels were measured as 84 ± 11, 76 ± 15 and 86 ± 26 % for the assays of MTT, Neutral Red and BrdU, corresponding viabilities of Latex were 10 ± 3, 4 ± 0 and 32 ± 11 %, with significant differences in statistics (Fig. 6). Thus, the HA hydrogels were considered as biocompatible.

Cell morphology on HA hydrogel surface

Morphologies of MC3T3 cells on the surfaces of the non-patterned and micro-patterned HA hydrogel were observed with a light microscope during *in vitro* cell culture for 7 days. At day 1, round-shaped cells were observed on the surfaces of both non-patterned and micro-patterned HA hydrogels. While the cells on the non-patterned HA hydrogel were observed as randomly distribution of adhered cells (Fig. 7a), those of the

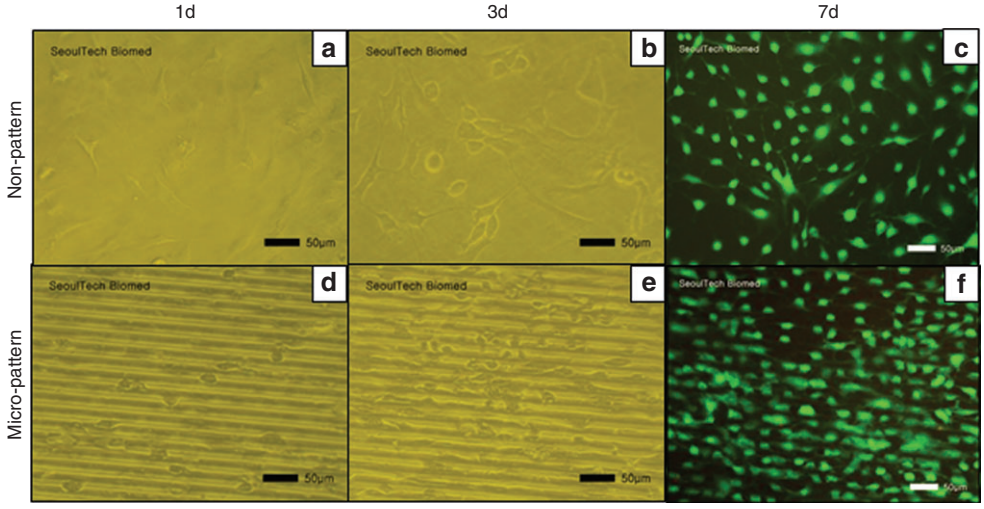

Fig. 7 Morphologies of MC3T3 cells on the surface of the non-patterned (a-c) and micro-patterned (d-f) HA hydrogel (×200) for 1 (a and d), 3 (b and e) and 7 day (c and f). The cells were seeded at a density of 50 000 cells per sample and cell viability was observed with Live & Dead assay (c and f).

micro-patterned one showed stable cell adhesions along the micro-patterns (Fig. 7d). At day 3, most of cells on both HA hydrogels were observed to be stretched. However, cellular behaviors between the HA hydrogels were clearly different depending on the employment of micro-patterns; i.e., the cells on the non-patterned HA hydrogel were observed to grow in the disorganized form, but those on the micro-patterned ones showed directed and organized cell growth along the micro-patterns side by side (Fig. 7b and e). Clearer distinctions of cell behaviors between the samples were observed after cell culture for 7 days. While the cells on the non-patterned HA hydrogel have grown up without the directional orders, those of the micro-patterned HA hydrogel proliferated better in both cell numbers and directions along lines of micro-patterns than those of the non-patterned did (data not shown).

To identify viability and morphology of the cells, a live & dead assay was performed with a fluorescence microscope at day 7, where live and dead cells were observed as green and red in color, respectively. All of the survived MC3T3 cells attached on both the micro-patterned/non-patterned HA hydrogel were seen in green. However, there were clear differences between the morphologies of MC3T3 cells on the non-patterned and micro-patterned hydrogels. Higher number of cell proliferation on the micro-patterned HA hydrogel was observed than that of the non-patterned one was, indicating that the micro-patterns on the HA hydrogel induced higher cell adhesion and proliferation (Fig. 7c and f). Furthermore, the cells on the non-patterned HA hydrogel randomly proliferated.

The HA hydrogels with MC3T3 cells cultured for 7 days were observed with SEM in order to evaluate cellular behaviors on both micro-patterned and non-patterned HA hydrogel (Fig. 8). Irregular star-shaped MC3T3 cells were observed on the surface of non-patterned HA hydrogel (Fig. 8b-d). However, MC3T3 cells on the micro-patterned HA hydrogel attached stably demonstrating higher degree of cell alignments along the micro-pattern lines (Fig. 8b-f-h). Spreading of the adhered MC3T3 cells was observed on the micro-patterns of the HA hydrogel. Particularly, most of the MC3T3 cells on the micro-patterned hydrogel were stretched thin and fine extracellular matrix to construct bone tissues, possibly, as indicated in arrow (Fig. 8c, d, g and h).

Histological observation of *in vitro* tissue-cultured HA hydrogel

Histologies of tissue regeneration of MC3T3 cells on the non-patterned and micro-patterned HA hydrogels were observed by processing of F-actins staining because MC3T3 cells differentiated for osteogenesis. To

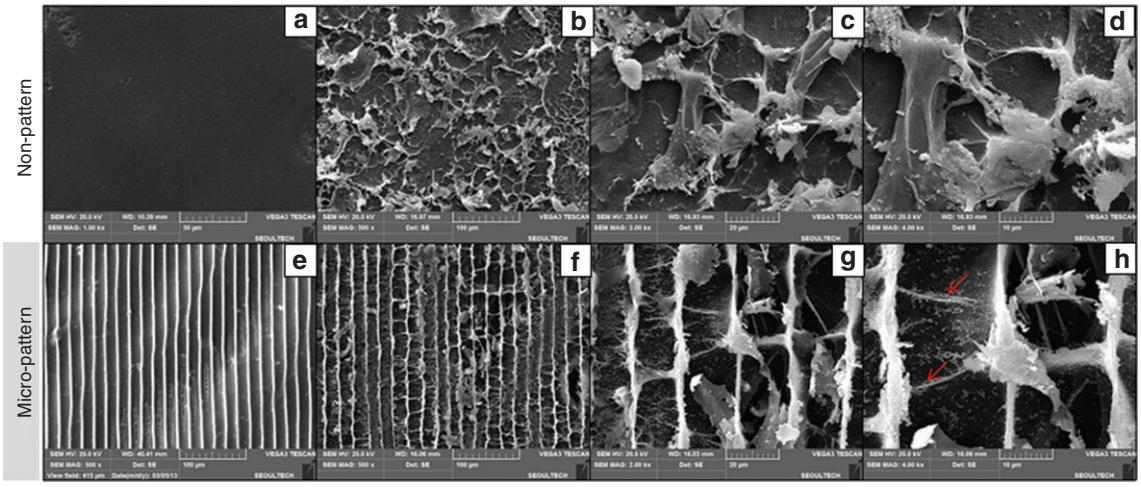

Fig. 8 SEM images of the cells on HA hydrogel surface with non-pattern (a-d) and micro-pattern (e-h), where the surface before (a and e; ×500), and after *in vitro* cell culture for 7 days [b-d and f-h; (b and f; ×500), (c and g; ×2000), (d and h; ×4000)]. The arrows indicated development of major cell spreading along the patterns on the micro-patterned hydrogel with development of extracellular matrix (ECM) to the interspace of micro-patterns. The cell spreading and ECM development on the non-patterned hydrogel were also observed for comparison with.

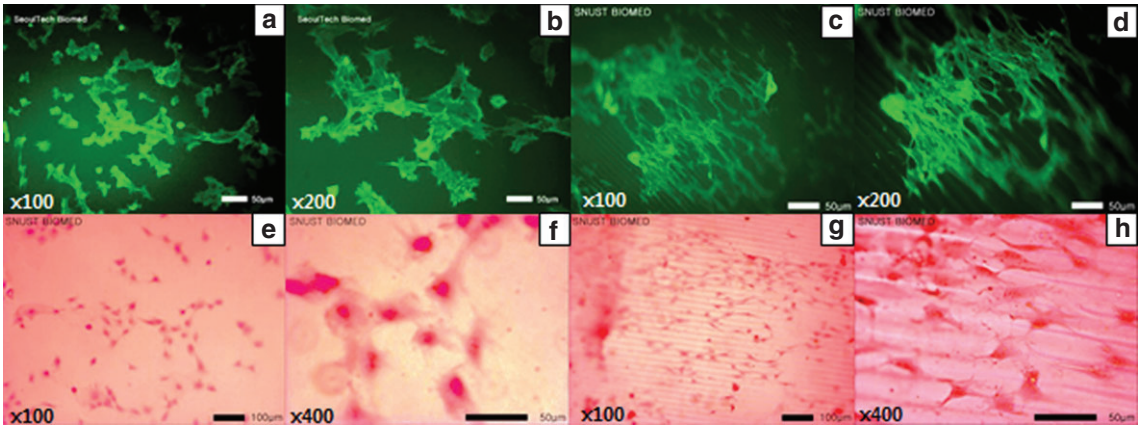

Fig. 9 Stainings of F-actin (a-d) and H&E (e-h) of the cells on the surface of HA hydrogel with non-pattern (a-b and e-f) and micro-pattern (c-d and g-h), where (a, c, e and g; ×100), (b and d; ×200) and (f and h; ×400)].

identify the development of F-actins of the MC3T3 cells on the micro-patterned and non-patterned hydrogel, we stained the regenerated tissue of the hydrogel after cell culture for 7 days. MC3T3 cells on the non-patterned HA hydrogel showed distribution of disorderly aggregates with F-actins (Fig. 9a and b), but those on the micro-patterned one showed formation of long stretches. F-actins of MC3T3 cells were generated on the micro-patterned HA hydrogel along the micro-patterns. Based on these results, we concluded that MC3T3 cells attached and proliferated on the micro-patterned HA hydrogel by developing F-actins along the pattern of the HA hydrogel (Fig. 9c and d).

Development of extracellular matrix was further observed by staining with H&E. When the MC3T3 cells were stained by H&E staining, the basophilic nuclei were stained in purple by hematoxylin, and acidic cytoplasm was counterstained in pink by eosin Y. MC3T3 cells grew randomly in aggregated shapes and attached disorderly on the surface of the non-patterned HA hydrogel (Fig. 9e and f), but the MC3T3 cells on the micro-patterned ones were distributed and observed to be stretched depending on the pattern of the HA hydrogel (Fig. 9g and h), as we have observed the morphologies in F-actin staining.

Discussion and conclusion

Micro-patterning of HA hydrogel was successfully fabricated by applications of micro-patterned PDMS substrates in the soft lithography as observed by SEM. The obtained micro-patterned hydrogel kept nearly the same dimension of the diameter and depth of the pattern as that of master, even after its swelling in water, only 17 % increase in the diameter of the micro-pattern after its immersion in the medium of *in vitro* cell culture for 7 days. The responses of MC3T3 cells were dependent on the employment of micro-patterning of the HA hydrogel, showing more adhesion and proliferation of MC3T3 cells on the micro-patterned hydrogel than that of the non-patterned one showed, as observed by the live & dead assay and stains of both F-actin and H&E. The proliferating cells were directed by the micro-patterning of the HA hydrogel and secreted more extracellular matrix as observed by H&E staining. On the contrary, less number of MC3T3 cells was attached and irregularly proliferated on the surfaces of the non-patterned HA hydrogel. Furthermore, the micro-patterned HA hydrogel showed excellent biocompatibility such as its minimal cytotoxicity as evaluated by the assays of MTT, BrdU and Neutral Red. Since the surface of non-patterned HA hydrogel has shown less adhesive properties due to its extreme hydrophilicity, the reasons of more initial cell adhesion on the micro-patterned HA hydrogel may be from the facts that the micro-patterns supplied the spaces for the seeding cells to adhere on. The patterns with approximately 20 μm diameter of the semi-circles and 8.5 μm in depth would be enough for the floating cells to adhere on, subsequently leading to more cell proliferation and tissue regeneration along the paths of the micro-patterns. Based on the results of cellular behaviors such as adhesion and proliferation

leading to tissue regeneration as well as biocompatibility, the micro-patterned, more cell-adhesive/proliferative HA hydrogel seemed to be an excellent candidate for a scaffold for tissue engineering compared to the non-patterned hydrogel with less cell adhesiveness.

Acknowledgments: This study was supported by the Research Program funded by the Seoul National University of Science and Technology (2014-0523).

Conflict of interest statement: This research does not have conflict of interest.

References

[1] E. Jang, S. Kim, W. G. Koh. *Biosens. Bioelectron.* **31**, 529 (2012).
[2] Y. Ma, J. Thiele, L. Abdelmohsen, J. Xu, W. T. S. Huck. *Chem. Commun.* **50**, 112 (2014).
[3] A. Weltin, K. Slotwinski, J. Kieninger, I. Moser, G. Jobst, M. Wego, R Ehret, G. A. Urban. *Lab. Chip* **14**, 138 (2014).
[4] N. T. Nguyen, S. A. M. Shaegh, N. Kashaninejad, D. T. Phan. *Adv. Drug Deliv. Rev.* **65**, 1403 (2013).
[5] D. A. Chang-Yen, R. K. Eich, B. K. Gale. *J. Lightwave Technol.* **23**, 2088 (2005).
[6] Y. Y. Huang, W. Zhou, K. J. Hsia, E. Menard, J. U. Park, J. A. Rogers, A. G. Alleyne. *Langmuir* **21**, 8058 (2005).
[7] Y. Huang, G. T. Paloczi, A. Yariv. *J. Phys. Chem. B* **108**, 8606 (2004).
[8] G. Ye, X. Wang. *Biosens. Bioelectron.* **26**, 772 (2010).
[9] M. E. Helgeson, S. C. Chapin, P. S. Doyle. *Curr. Opin. Colloid Interface Sci.* **16**, 106 (2011).
[10] K. Y. Suh, J. Seong, A. Khademhosseini, P. E. Laibinis, R. Langer. *Biomaterials* **25**, 557 (2004).
[11] G. Ye, X. Li, X. Wang. *Chem. Commun.* **46**, 3872 (2010).
[12] A. Khademhosseini, R. Langer. *Biomaterials* **28**, 5087 (2007).
[13] H. Yan, Y. Zhao, C. Qiu, H. Wu. *Actuator B-Chem.* **132**, 20 (2008).
[14] F. D. Benedetto, A. Biasco, D. Pisignano, R. Cingolani. *Nanotechnology* **16**, S165 (2005).
[15] P. Kim, K. W. Kwon, M. C. Park, S. H. Lee, S. M. Kim, K. Y. Suh. *BioChip J.* **2**, 1 (2008).
[16] H. Kenar, A. Kocabas, A. Aydinli, V. Hasirci. *J. Biomed. Mater. Res. A* **85A**, 4 (2007).
[17] J. M. Karp,Y. Yeo, W. Genga, C. Cannizarro, K. Yan, D. S. Kohane, G. V. Novakovic, R. S. Langer, M. Radisic. *Biomaterials* **27**, 4755 (2006).
[18] C. J. Pan, Y. D. Nie, Y. X. Dong. *Adv. Mater. Res.* **284–286**, 1815 (2011).
[19] J. Shaik, J. S. Mammed, M. J. McShane, D. K. Mills. *J. Med. Eng.* **2013**, 1 (2013).
[20] S. Moon, S. K. Hasan, Y. S. Song, F. Xu, H. O. Keles, F. Manzur, S. Mikkilineni, J. W. Hong, J. Nagatomi, E. Haeggstrom, A. Khademhosseini, U. Demirci. *Tissue Eng. Part C: Methods* **16**, 157 (2010).
[21] N. L'Heureux, N. Dusserre, G. Konig, B. Victor, P. Keire, T. N. Wight, N. A. F. Chronos, A. E. Kyles, C. R. Gregory, G. Hoyt, R. C. Robbins, T. N. McAllister. *Nat. Med.* **12**, 361 (2006).
[22] R. Mukherjee, A. Sharma, G. Patil, D. Faruqui,P. Sarathi, G. Pattader. *Bull. Mat. Sci.* **31**, 249 (2008).
[23] A.C. R. Grayson, R. S. Shawgo, A. M. Johnson, N. T. Flynn, Y. Li, M. J. Cima, R. Langer. *IEEE* **92**, 6 (2004).
[24] K. Morishima, Y. Tanaka, M. Ebara, T. Shimizu, A. Kikuchi, M. Yamato, T. Okano, T. Kitamori. *Sens. Actuators B Chem.* **119**, 345 (2006).
[25] G. D. Prestwich, D. M. Marecak, J. F. Marecek, K. P. Vercruysse, M. R. Ziebell. *J. Control Release* **53**, 93 (1998).
[26] G. Kogan, L. Šoltés, R. Stern, P. Gemeiner. *Biotechnol. Lett.* **29**, 17 (2007).
[27] K. Y. Lee, D. J. Mooney. *J. Am. Chem. Soc.* **101**, 1869 (2001).
[28] S. Choi S, W. Choi, S. Kim, S. Y. Lee, I. Noh, C. W. Kim. *Biomater. Res.* **18**, 6 (2014).
[29] R. U. Sidwell, A. P. Dhillon, P. E. M. Butler, M. H. A. Rustin. *Clin. Exp. Dermatol.* **29**, 630 (2004).
[30] N. J. Lowe, C.A. Maxwell, P. Lowe, M. G. Duickb, K. Shah. *J. Am. Acad. Dermatol.* **45**, 930 (2001).
[31] M. A. Koo, J. L. Kang, M. H. Lee, H. J. Seo, B. J. Kwon, K. E. You, M. S. Kim, D. Kim D, et al. *Biomater. Res.* **18**, 7 (2014).
[32] S. H. Kim, S. H. Kim, Y. H. Kim. *TERM* **3**, 13 (2006).
[33] J. Yeom, B. W. Hwang, D. J. Yang, H. I. Shin, S. K. Hahn. *Biomater. Res.* **18**, 8 (2014).
[34] Y. Son, J. Lee, Y. J. Choi, C. H. Kim, H. Kim. *TERM* **8**, 446 (2011).
[35] Y. S. Shin, J. S. Lee, J. W. Choi, B. H. Min, J. W. Chang, J. Y. Lim, C. H. Kim. *TERM* **9**, 203 (2012).
[36] J. A. Hubbell. *J. Control. Release* **39**, 305 (1996).
[37] K. Ghosh, X. D. Ren, X. Z. Shu, G. D. Prestwich, R. A. F. Clark. *Tissue Eng.* **12**, 601 (2006).
[38] G. H. Kim, Y. M. Kang, K. N. Kang, D. Y. Kim, H. J. Kim, B. H. Min, J. H. Kim, M. S. Kim. *TERM* **8**, 1 (2011).
[39] H. Yoon, S. G. Oh, D. S. Kang, J. M. Park, S. J. Choi, K. Y. Suh, K Char, H. H. Lee. *Nat. Commun.* **2**, 455 (2011).
[40] D. Kim, S. Kim, S. Jo, J. Woo, I. Noh. *Macromol. Res.* **19**, 573 (2011).
[41] D. Kim, S. Kim, S. Jo, J. Woo, I. Noh. *Macromol. Res.* **19**, 396 (2011).